Chemical Engineering Journal 165 (2010) 966–973

Contents lists available at ScienceDirect

Chemical Engineering Journal

journal homepage: www.elsevier.com/locate/cej

A novel combined manufacturing technique for rapid production of IRMOF-1 using ultrasound and microwave energies

Rana Sabouni, Hossein Kazemian, Sohrab Rohani*

Department of Chemical and Biochemical Engineering, The University of Western Ontario, Ontario, Canada N6A5B9

ARTICLE INFO

Article history:
Received 8 July 2010
Received in revised form 8 September 2010
Accepted 24 September 2010

Keywords:
Metal organic framework
IRMOF-1
Ultrasonic
Microwave
Surface area
Particles size and sample activation

ABSTRACT

The metal organic framework IRMOF-1 was successfully synthesized by applying a combination of ultrasonic (UTS) and microwave (MW) energy sources for rapid synthesis under various operating conditions including: sonication time and temperature as well as microwave irradiation time. Moreover sample activation was employed to improve surface area of the synthesized IRMOF-1. While the highest Langmuir surface area of the as-synthesized samples was 1315 m^2/g sample, surface area of the activated sample was 2473 m^2/g. The reaction products were characterized by X-ray diffraction (XRD), scanning electron microscope (SEM), solid-state Fourier transform infrared spectroscopy (FTIR), thermogravimetric analysis (TGA), and BET.

1. Introduction

In the last 10 years, metal organic frameworks materials (MOFs) have attracted tremendous interest amongst researchers in diverse science and technology areas, due to their outstanding properties including very large surface area, which is leading to wide varieties of potential industrial applications such as hydrogen storage technology [1]. MOFs are a new class of crystalline porous materials [2,3] composed of metal ions (or metal clusters) connected by means of multi-functional organic ligands (e.g. carboxylates, tetrazolate, sulfonates, etc.) in order to form a three-dimensional structure [4]. Remarkable improvements of the MOFs have been reported regarding their extremely high surface area and pore volume as well as high structural and chemical diversity, which can be achieved by changing the nature of organic linker and/or changing the connectivity of the inorganic moiety. For instances, the MOF-177 with surface area of 5640 m^2/g [5], MIL-101 with 5900 m^2/g [6], and UMCM-2 with 6000 m^2/g [7] are landmarks in this regard. The pore size of MOF materials is tuneable from microporous (i.e. Angstrom) to mesoporous (i.e. nanometer) scale [8–10].

There are hundreds of articles reporting new types of MOF materials; however IRMOF-1 is amongst the most well studied MOFs with promising industrialization potential. IRMOF-1 consisted of Zn_4O as metal clusters connected by 1, 4-benzenedicaboxylate (BDC) as a linear linkers to form a cubic network. Li et al. [2] were the first group who reported IRMOF-1 in 1999. Later on, many studies were carried out on the synthesis of this MOF using different carboxylate linker by means of classical solvothermal method [3], microwave radiation [11] and ultrasonic irradiation [12]. Furthermore, IRMOF-1 capability toward gas adsorption and storage including hydrogen storage [13], carbon dioxide adsorption (21.7 mmol CO_2/g or 290 cm^3 (STP)/cm^3) [14] were also investigated.

Potentially, MOF materials can be applied in numerous industrial applications including gas separation, adsorption and storage processes [15,16], heterogeneous catalysis [7], pharmaceutical manufacturing processes and drug delivery [10]. Carbon dioxide (CO_2) is one of the main green house gases, which is known for its harmful effect on global warming and climate change. Consequently, tremendous efforts have been intensified to reduce CO_2 emission into the atmosphere. At the present, removal of CO_2 from exhaust flues of power plants is primarily accomplished by means of solvent absorption using aqueous alkanolamine solvents or by cooling and pressurizing the exhaust gasses [17], which are costly and inefficient techniques having several other environmental issues including the alkanolamines volatility [18]. In this regards, MOF materials, which have shown remarkable adsorption selectivity and capacity for CO_2 capturing offer unique opportunities for CO_2 removal. According to the literature, one of the most effective MOF types for CO_2 adsorption is MIL-101 with a capacity of 40 mmol CO_2/g or 390 cm^3 (STP)/cm^3 [19] followed by MOF-177 with adsorption capacity of 33.5 mmol CO_2/g or 320 cm^3 (STP)/cm^3 [19].

---

* Corresponding author. Tel.: +1 519 661 4116; fax: +1 519 661 3498.
E-mail address: srohani@uwo.ca (S. Rohani).

1385-8947/$ – see front matter. Crown Copyright © 2010 Published by Elsevier B.V. All rights reserved.
doi:10.1016/j.cej.2010.09.036

Although there are large number of articles reporting synthesis of new types of MOFs, but few of them focused on optimizing the synthesis procedures in order to develop higher yield manufacturing techniques. Most of the MOFs are synthesised using classical solvothermal methods [20,21]. These methods require very long time of reaction (e.g. up to several days). However, because of the huge potential for industrial application of MOFs [1,22], it is important to develop novel and more efficient alternative synthesis techniques, which are techno-economically viable and capable for scaling up to larger industrial production scales. It is desirable to reduce costs of the final product by reducing synthesis time and increasing energy efficiency. In this respect, several alternative synthesis techniques such as solvent free method, microwave irradiation [11,23–25], electrochemical methods [26] and ultrasonic irradiation [10,12,27] have been reported. Interests toward the new techniques are attributed to their higher efficiency in terms of synthesis time and production yield as well as to their environmental friendly nature [28].

Although ultrasonic method has been widely employed in several research areas including biological cell-disruption, medical imaging, thermoplastic welding, waste treatment, food processing and pharmaceutical industries, so far, only a few articles have reported the utilization of ultrasonic energy to synthesize MOF materials. The ultrasonic synthesis of IRMOF-1 (MOF-5) was first reported in 2008 [12]. The ultrasonic irradiation accelerates the chemical reactions and initiates new reactions that are difficult to achieve under normal conditions [29,30]. In addition, ultrasound can lead to homogenous nucleation [31,32]. The main effect of ultrasound energy on the chemical synthesis arises from the acoustic cavitation phenomenon, which includes: creation, growth and collapse of bubble in liquid medium [33–35]. The collapse of the bubbles during cavitation phenomenon leads to very unique conditions such an extremely high local temperatures (i.e. local hot spots; 2500–5000 K), high pressures (i.e. >20 MPa), and very high cooling rates (i.e. $>10^7$ K s^{-1}) [23–25,36]. In addition, shock waves created by homogenous cavitation causes particle collisions in high velocities generating dramatic changes in their surface morphology, composition and reactivity [35].

Nowadays, microwave irradiation is known as a promising energy source for large scale production of materials. Microwave generates direct and uniform energy which can be absorbed throughout the entire volume of an object causing even and rapid heating. Furthermore, microwave leads to homogeneous nucleation, fast crystallization [37], diverse morphology/size [38], phase selectivity and reduction in particle size [24]. Choi et al. synthesized IRMOF-1 by means of microwave irradiation in 2008 [25]. Later in 2009, Lu et al. [11] demonstrated an improved microwave synthesis technique for synthesizing IRMOF-1 [25] and investigated its capability to capture CO_2.

The main objective of this work was to develop a novel hybrid manufacturing technique by applying a combination of both ultrasonic (UTS) and microwave (MW) irradiation to develop a rapid and more efficient procedure for synthesis of IRMOF-1. To the best of the authors' knowledge, this is the first time that a combination of UTS and MW energies is used for the synthesis of IRMOF-1 (MOF-5). The experimental parameters were optimized by means of statistical methods using a 3^2 factorial design with center points per block (i.e. 9 experiments in total). The synthesized samples were then characterized by means of different instrumental techniques including XRD, FTIR, TGA, and BET.

2. Materials and methods

Zinc(II) nitrate hexahydrate ($Zn(NO_3)_2{\cdot}6H_2O$, 99.5%) was purchased from J.T Baker, Phillipsburg, USA), Benzene-1,4-dicarboxylic acid (H_2BDC, 98%) and N,N-diethylformamide (DEF, 99%) were purchased from Alfa-Aesar (Jobson Matthey Company, Ward-Hill, USA). N,N-dimethylformamide (DMF, 99.9%) was purchased from Caledon Laboratory Chemicals (Georgtown, Ontario, Canada). Chloroform 99% was purchased from OmniSolv EMD Chemicals (Gibbstown, New Jersey, USA). All of the chemicals were used as purchased without any further purification. As ultrasonic bath (240 W, 50/60 Hz, Crest Ultrasonics, Malaysia and a microwave system (Daytron, 980 W, microwave frequency 2450 MHz, Korea) were used for synthesis purposes. Characterizations of the MOF samples were carried out by means of various instrumental techniques. The XRD data was collected using a Rigaku–MiniFlex powder diffractometer (Woodlands, USA), using CuK_α (λ for $K_\alpha = 1.54059$ Å) over the range of $5° < 2\theta < 40°$ with step width of 0.02° The SEM images were taken by JSM 600F model, Joel, Japan operating at 10 keV of acceleration voltage. The FTIR spectra were recorded on solid state by a Bruker Vector 22 (Milton, Ontario, Canada). The sample scan time was 32 s over the 400–4000 cm^{-1} spectral region with resolution of 4 (cm^{-1}). The thermal analyses were performed using a Mettler Toledo TGA/SDTA 851^e model (Mississauga, ON, Canada) with version 6.1 Star^e software. The samples were heated from 25 °C to 600 °C at heating rate of 10 °C/min under nitrogen purge (50 mL/min). Surface area and pore size of the samples were measure by means of a BET analyzer (Micrometrics ASAP 2010). Known amounts of samples (e.g. 50–80 mg) were loaded into the BET sample tube and degassed under vacuum (10^{-5} Torr) at 125 °C for 6 h. The Langmuir model was applied to measure the specific surface area of the prepared samples.

2.1. Synthesis

The IRMOF-1 samples were synthesized with the same batch composition reported by Millward and Yaghi [14], while some minor modifications were also applied. In the first stage for evaluation of the classical hydrothermal synthesis by means of a electrical oven (OV), a IRMOF-1 sample was synthesized as following: in a 100 mL beaker, 0.947 g of Zn $(NO_3)_2{\cdot}6H_2O$ and 0.176 g of H_2BDC were dissolved in 10 mL of DEF. Then the resultant solution was transferred into a 25 mL Teflon reactor with a tight cap and kept at 100 °C for 20 h. The product crystallites were then washed four times with fresh DMF (40 ml). For two step synthesis (UTS and MW), the same batch composition as of the classical synthesis was used, however, the energies sources for heating were UTS and MW irradiations instead of electrical oven. After mixing and dissolving the reactants, the clear solution was transferred into a 25 mL Teflon reactor and irradiated in the ultrasonic bath for specific sonication time at the predetermined temperature according to the experimental design (see Table 1). The sonified samples were then irradiated in a microwave oven for various irradiation times depending to the sonication condition (see Table 1). The produced solid phase was then filtered and washed four times with fresh DMF (40 mL) and dried at room temperature. The investigated parameters for ultrasonic energy were sonication time (i.e. 15 min, 1 h and 3.5 h) and ultrasonic bath temperature (i.e. 25 °C, 52 °C and 80 °C).

Sample activation was investigated to improve surface area and pore volume of the synthesized IRMOF-1 samples. Solvent exchange was employed as activation method. Solvent exchange techniques are often used to remove guest molecules (i.e. DEF in our study). It is noteworthy to mention that boiling point and polarity of the solvent must be considered in order not to damage the original framework. Some of the synthesized samples were exposed to fresh chloroform for three times in 72 h. The solvent exchanged IRMOF-1 samples were dried in an electrical oven at 70 °C for 1 h. The activated products were then immediately transferred into desiccators in order to minimize exposure to humidity and other contaminants form air.

Table 1
Experimental design for as-synthesized samples, effect of ultrasonic bath temperature and time.

Sample code	UTS time (h)	UTS Temperature (°C)	MW time (s)	Langmuir surface area (m^2/g)	Particles size (μm)
IRMOF-1 (S1)	0.25	RT	120	79	11
IRMOF-1 (S2)	0.25	52	90	903	9
IRMOF-1 (S3)	0.25	80	85	549	12
IRMOF-1 (S4)	1.8	RT	190	780	12
IRMOF-1 (S5)	1.8	52	93	420	8
IRMOF-1 (S6)	1.8	80	73	954	7
IRMOF-1 (S7)	3.5	RT	150	162	8
IRMOF-1 (S8)	3.5	52	100	289	6
IRMOF-1 (S9)	3.5	80	83	1315	5

Table 2
Comparison of various preparation methods of IRMOF-1.

Reference	Nitrogen uptake (mmol/g)	BET surface area (m^2/g)	Langmuir surface area (m^2/g)
[40]	23.3	1810	2160
[41]	11.8	572	1014
[42]		1100	
[43]		773	
[44]		1300	
[2]	29.7		2900
[45]			3080
[13]	44.5	3800	4400
S2 (this study)		1874	2473

Studies have shown that, various parameters including synthesis condition (i.e. linker and metal centers, solvent, source of heating, time and temperature, pressure, etc.), activation procedure, type of solvent used for sample activation (solvent exchange), as well as storage condition can remarkably affect the surface area of MOFs materials [39]. For instance, using DMF as an alternative cheaper solvent to DEF, has resulted in MOFs products with lower surface areas [13]. Moreover, increasing the temperature and extending the synthesis reaction time caused yellow crystals to be produced with lower surface areas [13]. Literature data for the surface area of IRMOF-1 (MOF-5) along with data obtained in this research are compared in Table 2. It is obvious that preparation methods can remarkably influence the MOF surface area. According to the literatures data, the reported Langmuir surface areas for IRMOF-1 are in the range of 1014–4400 m^2/g, where the Langmuir surface area we achieved in this work (i.e. 2473 m^2/g) is in that range.

2.2. Experimental design

In order to optimize the IRMOF-1 production condition by means of the novel combined UTS + MW technique, a statistical approach using a 3^2 factorial design with center points per block we considered. Design-Expert 7.1.5 software (StatEase, Minneapolis, USA) was employed to investigate the effect that ultrasonic bath temperature and sonication time on the microwave irradiation time and consequently on the morphology, surface area and particle size and distribution of the synthesized IRMOF-1 samples The details of the factor levels employed for the experimental design and the responses examined in the study are summarized in Table 1.

The analysis of variance (ANOVA) was used to investigate which factors significantly influenced the microwave irradiation time and consequently the Langmuir surface area, and particle size. It was found that both investigated factors (i.e. UTS time and UTS temperature) strongly influence the final product microwave irradiation as well as particle size. However, these two factors were shown less effects on Langmuir surface area. Therefore, both particle size and microwave irradiation time were statistically analyzed using Design Expert 7.1.5 software by carrying data transformation (inverse transformation) to create strong model with a probability greater than *F*-value less than 0.05. The *F*-value was 19.38 for the inverse transformation of particle size data compared to an *F*-value of 5.69 for data without any transformation. An *F*-value of 10.99 was obtained when applying inverse transformation of the microwave data, and an *F*-value equal to 4.34 for the data without any transformation. The input factors were coded alphabetically (i.e. A for UTS time and B for UTS bath temperature). The two input factor interaction terms were coded by combining the main factors; AB for UTS time and UTS temperature interaction. The model was constructed by step-wise backward elimination of the statistically insignificant factorial terms and non-hierarchical terms. The final model for the particle size data is presented in Tables 3 and 5. In addition, final model of the microwave time data are summarized in Tables 4 and 5.

According to the data in Table 3, it can be concluded that IRMOF-1 particle size is affected by both ultrasonic temperature and time. The higher *F*-value (36.2) of the sonication time indicates that particle size is strongly affected by sonication time rather than ultrasonic temperature with an *F*-value of 13.87. Therefore, as sonication time increases, particle size decreases. In addition, particle size decreases as ultrasonic temperature increases. On the other hand, microwave irradiation time is strongly affected by ultrasonic temperature (*F*-value = 31.88). Increasing ultrasonic temperature reduces the microwave irradiation time during synthesis of IRMOF-1 crystallites as is shown in Table 4.

3. Results and discussion

3.1. As-synthesized samples

The IRMOF-1 crystallites synthesized by means of the novel hybrid two steps technique using UTS followed by MW irradiation

Table 3
Summary of the analysis of variance of the model equation of the particles size as function of synthesis variable.

Source	Sum of squares	Degree of freedom	Mean square	*F*-value	Prob > *F*-value
Model	0.0115	3	0.0038	19.3757	0.0035
A-UTS time	0.0072	1	0.0072	36.5026	0.0018
B-UTS temp	0.0027	1	0.0027	13.8761	0.0136
AB	0.0017	1	0.0017	8.5190	0.0331
Std. dev.	0.0141		R^2	0.9208	
Mean	0.1254		Adj-R^2	0.8733	
Pred-R^2	0.7631		Adeq. precision	11.9524	

Table 4
Summary of the analysis of variance of the model equation of the microwave time as function of synthesis variable.

Source	Sum of squares	Degree of freedom	Mean square	*F*-value	Prob > *F*-value
Model	5.1317E−05	3	1.7106E−05	10.9856	0.0122
A-UTS time	1.0102E−06	1	1.0102E−06	0.6488	0.4571
B-UTS temp	4.9650E−05	1	4.9650E−05	31.8865	0.0024
AB	8.3259E−07	1	8.3259E−07	0.5347	0.4974
Std. dev.	1.2478E−03			R^2	0.8683
Mean	9.9598E−03			Adj-R^2	0.7892
Pred-R^2	4.3504E−01			Adeq. precision	8.0178

Table 5
Final model equations for particles size and microwave time parameters.

Parameter	Model equations
Particles size	$\frac{1}{\mathrm{PS}} = 0.13 + 0.035A + 0.021B + 0.021AB$
Microwave time	$\frac{1}{\mathrm{MW\,(time)}} = 9.9966 \times 10^{-3} - 4.098 \times 10^{-4}A + 2.877 \times 10^{-3}B + 4.553 \times 10^{-4}AB$

A, sonication time; *B*, ultrasonic temperatuer; PS, particles size; MW (time), microwave irradiation time.

sources were compared with those of synthesized by means of the conventional solvothermal method using an electrical oven (OV) to confirm the existence of IRMOF-1 crystalline phase. The XRD patterns of some of the samples synthesized under the hybrid technique at different experimental conditions are illustrated in Fig. 1. According to the XRD patterns, most of the peaks match well with those for IRMOF-1 [10,12,13,29]. The main peak at $2\theta = 9.88^\circ$ ascertain the formation of IRMOF-1 crystalline phase which appears in all samples. In addition, two other peaks at $2\theta = 7.30^\circ$ and 14.02° appear in all samples because of microwave heating process which is consistent with other literatures [48,49]. Moreover, sample 4 and 6 shows an extra peak at $2\theta = 8.8^\circ$ in addition to the three characteristic peaks, which indicates that these two samples are a mixture of IRMOF-1 and an unidentified crystalline phase [11]. However, it can be seen that the XRD pattern of OV sample is slightly different. In this study, several trials were performed to synthesize IRMOF-1 using the classical oven technique, but none of them were successful (3 trials) even though the same procedure as of Millward et al. [14] was followed. This phenomenon has been reported previously [10]. Fig. 2 illustrates the SEM images of IRMOF-1 samples synthesized by means of the hybrid technique of UTS and MW. The IRMOF-1 morphology is characterized by typical cubic-shaped crystals with approximate dimensions of 5–15 μm. It can be observed that the IRMOF-1 crystallites synthesized under UTS and MW method (see Fig. 2(a)) are more regulated cubic shaped comparing to those synthesized with OV (see Fig. 1(b)). In addition, the IRMOF-1 synthesized by UTS and MW produced particles with a size reduction by a magnitude of approximately 10 comparing to those produced by oven. This reduction in particle size is common among crystals prepared using microwave or ultrasonic irradiations [32,46]. Moreover, particles size decreased with increasing ultrasonic bath temperature and sonication time (see Section 2.2). This can be attributed to the combination effects of ultrasonic and microwave irradiation as discussed earlier, where UTS and MW irradiations promote uniform and fast nucleation [47,48]. As a result, it can be concluded that using the two step synthesis method (UTS and MW) has produced IRMOF-1 with a higher quality than those synthesized by OV method [11]. It can be concluded that combination of ultrasonic and microwave irradiation provides a unique and promising method for the synthesis of MOFs.

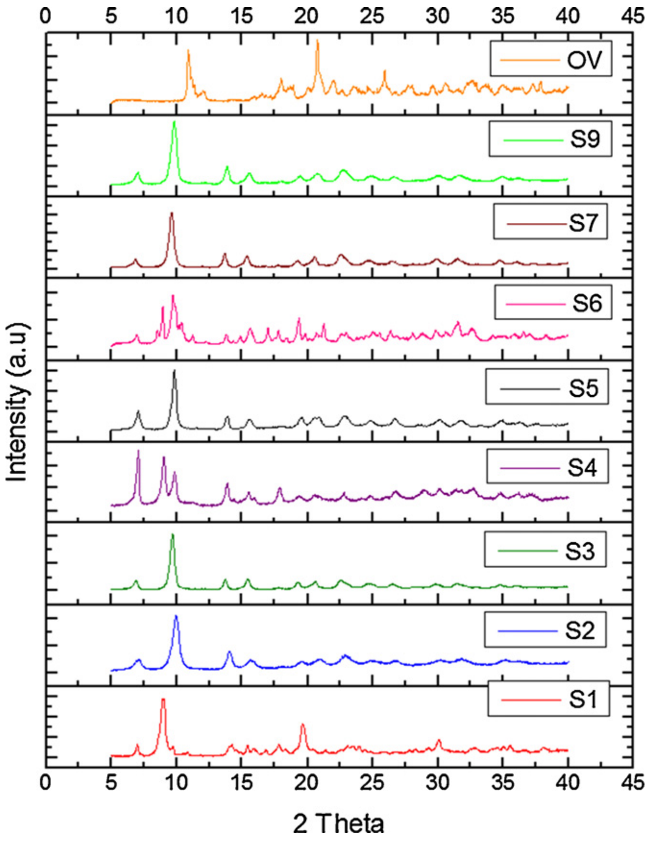

Fig. 1. XRD patterns for IRMOF-1 samples.

Fig. 3 illustrates the FTIR spectra of IRMOF-1 samples synthesized at different experimental conditions using the two step

Table 6
Effect of activation (solvent exchange).

Sample code	UTS (h)	UTS (°C)	MW (s)	Activation	Langmuir surface area (m^2/g)
S10 as	0.5	80	85	None	1370
S10 Act	0.5	80	85	Solvent exchange (chloroform three times for 3 days and later dry in oven at 70 °C for 1 h)	1723
S9 As	3.5	80	83	None	1315
S9 Act	3.5	80	83	Solvent exchange (chloroform three times for 3 days and later dry in oven at 70 °C for 1 h)	1786
S2 As	0.25	52	90	None	903
S2 Act	0.25	52	90	Solvent exchange (chloroform three times for 3 days and later dry in oven at 70 °C for 1 h)	2473

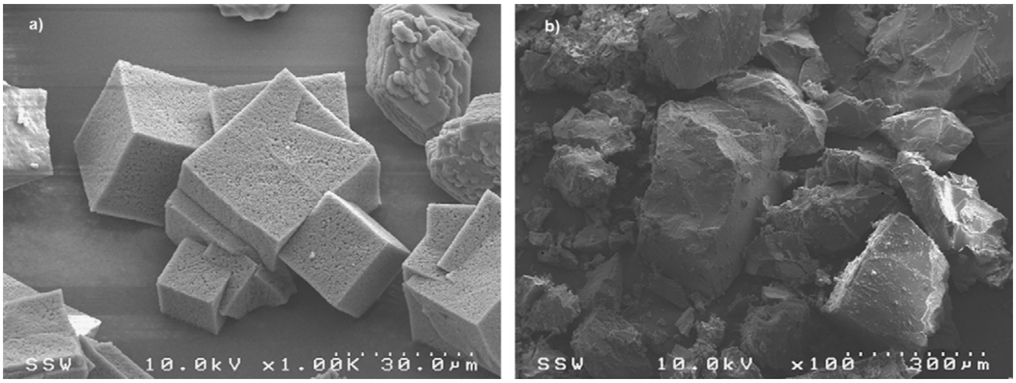

Fig. 2. SEM for sample 3 (a), and sample OV (b).

technique. The FTIR spectrums are in good agreement with the literature [49]. The vibration bands at 1400–1700 cm^{-1} represent the carboxylic functional group (COO). The vibration bands at 1608–1540 cm^{-1} and 1410–1340 cm^{-1} can be assigned to the symmetric and asymmetric vibrations of BDC [50]. The two absorptions bands located at 1572 cm^{-1} and 1506 cm^{-1} belong to the carboxylic (COO) asymmetric stretching, whereas the band at 1391 cm^{-1} can be assigned to the corresponding symmetric stretching vibration. The vibration bands at 700–1200 cm^{-1} can be considered as the fingerprint of terephthalate compounds. The absorption peak at 530 cm^{-1} is relevant to the secondary building unit (SBU) of IRMOF-1, which represents the (Zn–O) vibration of tetrahedral coordinated Zn_4O cluster. The vibration peaks of at 3500–3200 cm^{-1} correspond to the OH group of the adsorbed water molecules [50].

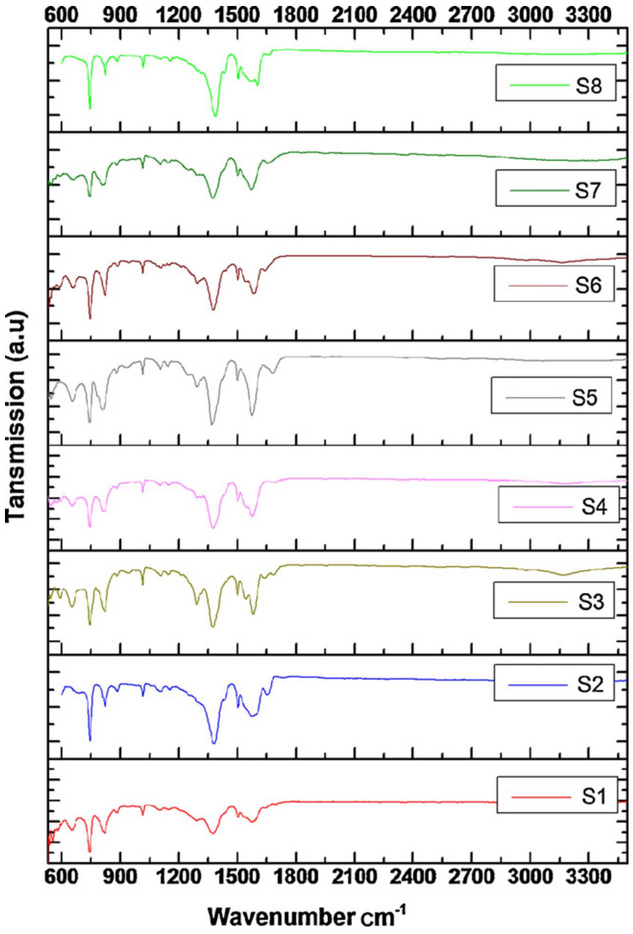

Fig. 3. FTIR spectra of IRMOF-1 samples.

Fig. 4 illustrates the TGA curves of the IRMOF-1 samples synthesized in this study by means of the hybrid technique. Thermal analysis results revealed that the overall thermal stability of the samples is similar to those reported in the literatures [14,44,25]. TGA curves show two distinguished weight loses. The first gentle slope of weight loss occurs between 100–250 °C (ca. 20%) and corresponds to the evaporation of trapped DEF and DMF and adsorbed water molecules [51]. This amount of non-volatile DEF and DMF is trapped inside the IRMOF-1 samples during the crystallization period and washing process. The second sharp weight loss occurs between 420 and 500 °C (ca. 38%), which is attributed to decomposition of IRMOF-1 structure [14].

In this study, the Langmuir surface area of IRMOF-1 as-synthesized (i.e. without any activation) for the two steps synthesis

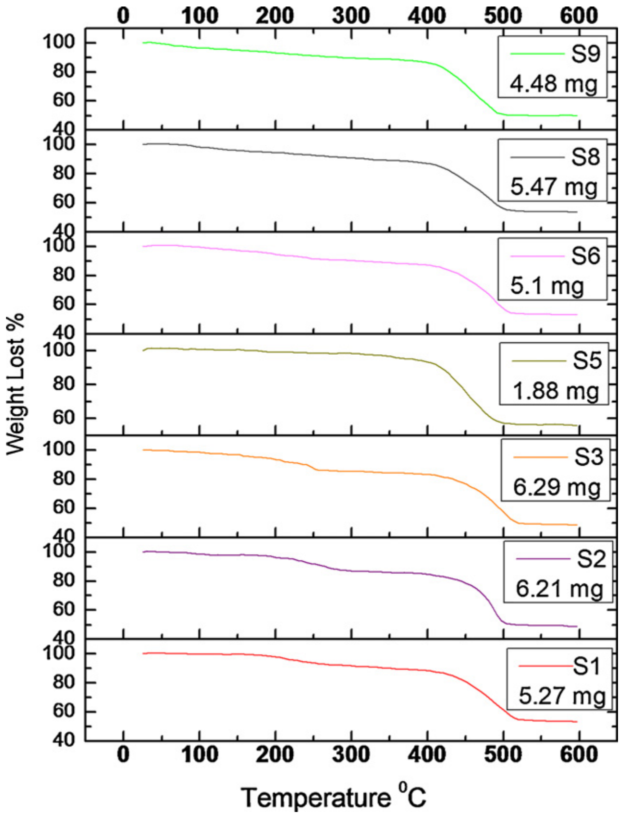

Fig. 4. Thermogravimetric analysis results for IRMOF-1 samples, the heating rate of all samples was 10 °C/min and the atmosphere was N_2.

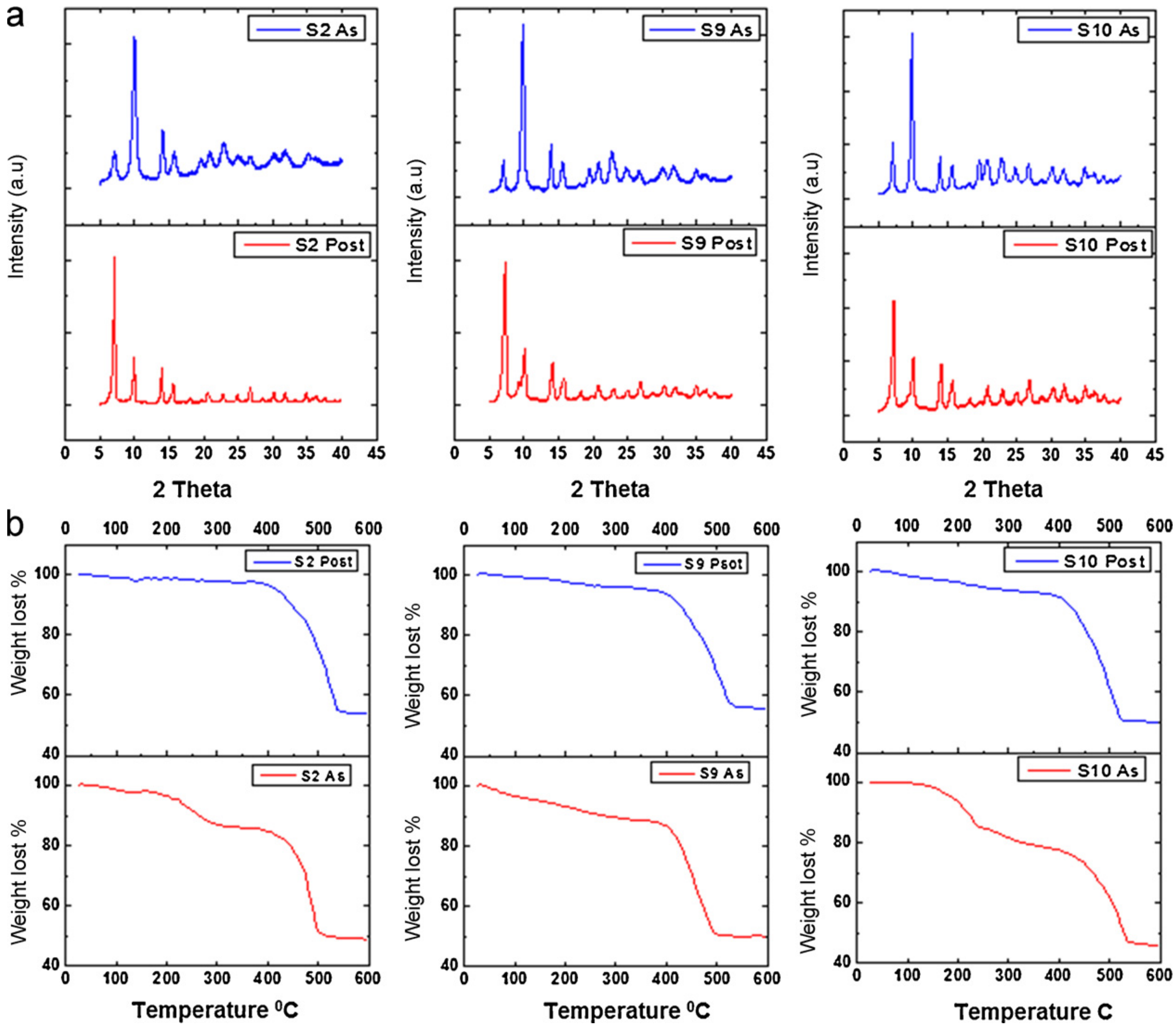

Fig. 5. (a) XRD comparison between as-synthesized samples and activated samples, (b) TGA comparison between as-synthesized samples and activated samples.

(UTS + MW) technique, was between 79 and 1315 m^2/g. The lower surface area of the sample in the present work can be attributed not only to the presence of Zn species in the pores [39,40], but also to the different condition applied for synthesis. However, the Langmuir surface area of the IRMOF-1 synthesized in the two steps (UTS + MW) technique, was increased radically for the activated samples (three times solvent exchange with chloroform in 72 h) (see Section 3.2)

3.2. Sample activation (solvent exchange)

The XRD patterns of the as-synthesized IRMOF-1 samples (i.e. S2, S9 and S10) and their corresponding activated samples are compared in Fig. 5(a). The XRD patterns have the same patterns, however, they show a slight difference in the peak intensity of both samples. The peaks at $2\theta = 7.9^\circ$ increased significantly and peaks at $2\theta = 9.89^\circ$ decreased for the samples that had under-

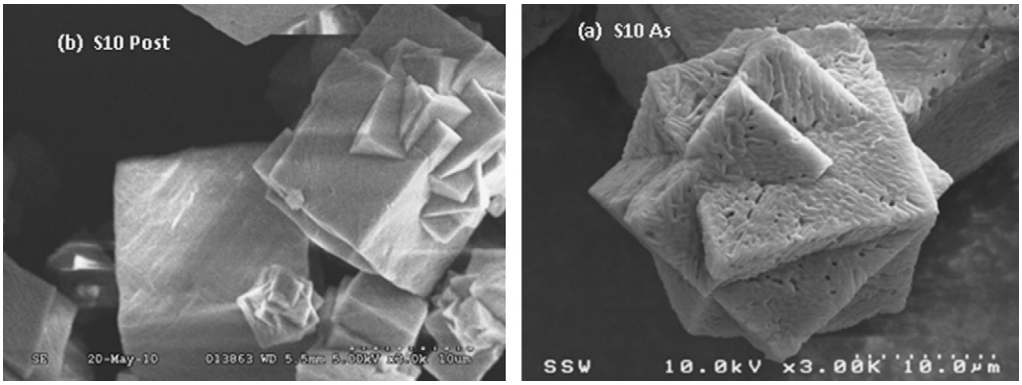

Fig. 6. SEM comparison between as-synthesized samples and activated.

gone solvent exchange with chloroform [11]. The difference in peaks intensity can be attributed to the removal of guest molecules during solvent exchange [11]. Moreover the SEM images illustrate changes in the surface roughness for the activated samples (as shown in Fig. 6). However, thermal analysis results show the changes between the as-synthesized and the modified samples. TGA curves in Fig. 5(b) show different thermal pattern between the as-synthesized and activated samples. The TGA curves corresponding to the as-synthesized samples show two distinct weight losses stages at 100–250 °C and 420–500 °C, however, in the activated sample the first gentle weight loss almost disappears and the samples show a steady continuous weight loss up to ca. 420 °C followed by a sharp weight loss at 430–500 °C. The disappearing of first small drop in weight loss can be related to the solvent exchange with chloroform and the way the samples were stored inside desiccators to minimize exposure to air and humidity.

The highest Langmuir surface area achieved in this study for the activated sample was 2473 m^2/g, which is in the range of the previously reported values using conventional oven method (see Tables 2 and 6). On the other hand, to the best of the authors' knowledge, 2473 m^2/g can be considered as the highest Langmuir surface area reported for alternative synthesis methods such as microwave irradiation. Lu et al. [11] have reported a successful synthesis of IRMOF-1 with 1263 m^2/g Langmuir surface area using microwave irradiation only. This improvement in the surface area can be attributed to the removal of guest molecules (e.g. DEF and DMF), which can be achieved by means of solvent exchange with fresh chloroform [11].

4. Conclusions

A novel hybrid synthesis technique based on a combined application of ultrasound and microwave energies was developed for rapid synthesis of IRMOF-1. The metal organic framework of IRMOF-1 ($Zn_4O(BDC)_3$) was successfully synthesized by means of the developed two step combined technique. This rapid manufacturing method showed promising results in terms of particles size distribution (lower particles size (5 μm, and narrower size distribution), morphology (more constructed crystallites) and surface area (higher surface area 2473 m^2/g) of the synthesized IRMOF-1 crystallites. Particle size of the samples synthesized by means of this novel hybrid technique was smaller in order of 10 μm in comparison to the classical solvothermal synthesis method (e.g. solvothermal oven synthesis). Furthermore, it can be concluded that the solvent exchange activation of IRMOF-1 synthesized by means of the combined techniques plays a very essential role to improve surface area of the MOF final product.

Acknowledgements

The authors wish to express their appreciation to the Natural Sciences and Engineering Research Council (NSERC) of Canada for financial support. They also would like to acknowledge the assistance of the Engineering Stores and the University Machine Services (UMS) at the University of Western Ontario.

References

[1] K.L. Lim, H. Kazemian, Z. Yaakob, W.R.W. Daud, Solid state materials and methods for hydrogen storage: a critical review, Chem. Eng. Technol. 33 (2) (2010) 1–15.
[2] H. Li, M. Eddaoudi, M. O'Keeffe, O.M. Yaghi, Design and synthesis of an exceptionally stable and highly porous metal-organic framework, Nature 402 (6759) (1999) 276–279.
[3] M. Eddaoudi, J. Kim, N. Rosi, D. Vodak, J. Wachter, M. O'Keeffe, et al., Systematic design of pore size and functionality in isoreticular MOFs and their application in methane storage, Science 295 (5554) (2002) 469–472.
[4] J.R. Long, O.M. Yaghi, The pervasive chemistry of metal-organic frameworks, Chem. Soc. Rev. 38 (5) (2009) 1213–1214.
[5] H.K. Chae, D.Y. Siberio-Pérez, J. Kim, Y. Go, M. Eddaoudi, A.J. Matzger, et al., A route to high surface area, porosity and inclusion of large molecules in crystals, Nature 427 (6974) (2004) 523–527.
[6] C. Férey, C. Mellot-Draznieks, C. Serre, F. Millange, J. Dutour, S. Surblé, et al., Chemistry: a chromium terephthalate-based solid with unusually large pore volumes and surface area, Science 309 (5743) (2005) 2040–2042.
[7] K. Koh, A.G. Wong-Foy, A.J. Matzger, A porous coordination copolymer with over 5000 m^2/g BET surface area, J. Am. Chem. Soc. 131 (12) (2009) 4184–4185.
[8] G. Férey, Hybrid porous solids: past, present, future, Chem. Soc. Rev. 37 (1) (2008) 191–214.
[9] O.M. Yaghi, M. O'Keeffe, N.W. Ockwig, H.K. Chae, M. Eddaoudi, J. Kim, Reticular synthesis and the design of new materials, Nature 423 (6941) (2003) 705–714.
[10] E. Haque, N. Khan, H.J. Park, S.H. Jhung, Synthesis of a metal-organic framework material, iron terephthalate, by ultrasound, microwave, and conventional electric heating: a kinetic study, Chem. – Eur. J. 16 (3) (2010) 1046–1052.
[11] C. Lu, J. Liu, K. Xiao, A.T. Harris, Microwave enhanced synthesis of MOF-5 and its CO_2 capture ability at moderate temperatures across multiple capture and release cycles, Chem. Eng. J. 156 (2) (2010) 465–470.
[12] Son W-, J. Kim, J. Kim, W-. Ahn, Sonochemical synthesis of MOF-5, Chem. Commun. (47) (2008) 6336–6338.
[13] S.S. Kaye, A. Dailly, O.M. Yaghi, J.R. Long, Impact of preparation and handling on the hydrogen storage properties of Zn_4O (1,4-benzenedicarboxylate)$_3$ (MOF-5), J. Am. Chem. Soc. 129 (46) (2007) 14176–14177.
[14] A.R. Millward, O.M. Yaghi, Metal-organic frameworks with exceptionally high capacity for storage of carbon dioxide at room temperature, J. Am. Chem. Soc. 127 (51) (2005) 17998–17999.
[15] Li J-, R.J. Kuppler, H-. Zhou, Selective gas adsorption and separation in metal-organic frameworks, Chem. Soc. Rev. 38 (5) (2009) 1477–1504.
[16] R.E. Morris, P.S. Wheatley, Gas storage in nanoporous materials, Angew. Chem. – Int. Ed. 47 (27) (2008) 4966–4981.
[17] N.H. Florin, A.T. Harris, Enhanced hydrogen production from biomass with in situ carbon dioxide capture using calcium oxide sorbents, Chem. Eng. Sci. 63 (2) (2008) 287–316.
[18] J. Johnson, Government and policy: putting a lid on carbon dioxide, Chem. Eng. News 82 (51) (2004), 36,38, 40, 42.
[19] P.L. Llewellyn, S. Bourrelly, C. Serre, A. Vimont, M. Daturi, L. Hamon, et al., High uptakes of CO_2 and CH_4 in mesoporous metal-organic frameworks MIL-100 and MIL-101, Langmuir 24 (14) (2008) 7245–7250.
[20] L- Qiu, A- Xie, L-. Zhang, Encapsulation of catalysts in supramolecular porous frameworks: Size- and shape-selective catalytic oxidation of phenols, Adv. Mater. 17 (6) (2005) 689–692.
[21] O.M. Yaghi, H. Li, T.L. Groy, Construction of porous solids from hydrogen-bonded metal complexes of 1,3,5-benzenetricarboxylic acid, J. Am. Chem. Soc. 118 (38) (1996) 9096–9101.
[22] U. Mueller, M. Schubert, F. Teich, H. Puetter, K. Schierle-Arndt, J. Pastré, Metal-organic frameworks – prospective industrial applications, J. Mater. Chem. 16 (7) (2006) 626–636.
[23] Z. Ni, R.I. Masel, Rapid production of metal-organic frameworks via microwave-assisted solvothermal synthesis, J. Am. Chem. Soc. 128 (38) (2006) 12394–12395.
[24] S.H. Jhung, J. Lee, J.W. Yoon, C. Serre, G. Férey, J. Chang, Microwave synthesis of chromium terephthalate MIL-101 and its benzene sorption ability, Adv. Mater. 19 (1) (2007) 121–124.
[25] Choi J-, Son W-, J. Kim, W-. Ahn, Metal-organic framework MOF-5 prepared by microwave heating: Factors to be considered, Micropor. Mesopor. Mater. 116 (1–3) (2008) 727–731.
[26] A. Pichon, A. Lazuen-Garay, S.L. James, Solvent-free synthesis of a microporous metal-organic framework, CrystEngComm. 8 (3) (2006) 211–214.
[27] Li Z-, Qiu L-, T. Xu, Y. Wu, W. Wang, Wu Z-, et al., Ultrasonic synthesis of the microporous metal-organic framework $Cu_3(BTC)_2$ at ambient temperature and pressure: an efficient and environmentally friendly method, Mater. Lett. 63 (1) (2009) 78–80.
[28] L- Qiu, Z- Li, Y. Wu, W. Wang, T. Xu, X. Jiang, Facile synthesis of nanocrystals of a microporous metal-organic framework by an ultrasonic method and selective sensing of organoamines, Chem. Commun. (31) (2008) 3642–3644.
[29] K- Kim, K-. Kim, Ultrasound assisted synthesis of nano-sized lithium cobalt oxide, Ultrason. Sonochem. 15 (6) (2008) 1019–1025.
[30] K.S. Suslick, Sonochemistry, Science 247 (4949) (1990) 1439–1445 (cited 10 May 2010).
[31] K.S. Suslick, S. Choe, A.A. Cichowlas, M.W. Grinstaff, Sonochemical synthesis of amorphous iron, Nature 353 (6343) (1991) 414–416.
[32] A. Gedanken, Using sonochemistry for the fabrication of nanomaterials, Ultrason. Sonochem. 11 (2) (2004) 47–55.
[33] K.S. Suslick, D.A. Hammerton, R.E. Cline Jr., The sonochemical hot spot, J. Am. Chem. Soc. 108 (18) (1986) 5641–5642.
[34] K.S. Suslick, T. Hyeon, M. Fang, J.T. Ries, A.A. Cichowlas, Sonochemical synthesis of nanophase metals, alloys and carbides, Mat. Sci. Forum 225–227 (PART 2) (1996) 903–912.
[35] R. Hiller, S.J. Putterman, B.P. Barber, Spectrum of synchronous picosecond sonoluminescence, Phys. Rev. Lett. 69 (8) (1992) 1182–1184.
[36] K.S. Suslick, The mechanochemical effects of ultrasound, Proc. First Int. Conf. 1 (1994) 43–49.

[37] J. Liu, A.T. Harris, Microwave-assisted acid digestion of alumina-supported carbon nanotubes, Sep. Purif. Technol. 62 (3) (2008) 602–608.

[38] S.H. Jhung, J- Chang, Y.K. Hwang, S-. Park, Crystal morphology control of AFI type molecular sieves with microwave irradiation, J. Mater. Chem. 14 (2) (2004) 280–285.

[39] N.L. Rosi, M. Eddaoudi, D.T. Vodak, J. Eckert, M. O'Keeffe, O.M. Yaghi, Hydrogen Storage in Microporous Metal-Organic Frameworks, Science 300 (2003) 1127–1129.

[40] S.J. Yang, J.Y. Choi, H.K. Chae, J.H. Cho, K.S. Nahm, C.R. Park, Preparation and enhanced hydrostability and hydrogen storage capacity of CNT©MOF-5 hybrid composite, Chem. Mater. 21 (9) (2009) 1893–1897.

[41] B. Panella, M. Hirscher, Hydrogen physisorption in metal-organic porous crystals, Adv. Mater. 17 (2005) 538.

[42] D. Farrusseng, C. Daniel, C. Gaudillère, U. Ravon, Y. Schuurman, C. Mirodatos, et al., Heats of adsorption for seven gases in three metal-organic frameworks: Systematic comparison of experiment and simulation, Langmuir 25 (13) (2009) 7383–7388.

[43] Z. Gu, D. Jiang, H. Wang, X. Cui, X. Yan, Adsorption and separation of xylene isomers and ethylbenzene on two Zn-terephthalate metal-organic frameworks, J. Phys. Chem. C 114 (1) (2010) 311–316.

[44] Y. Yoo, Z. Lai, H-. Jeong, Fabrication of MOF-5 membranes using microwave-induced rapid seeding and solvothermal secondary growth, Micropor. Mesopor. Mater. 123 (1–3) (2009) 100–106.

[45] A. Dailly, J.J. Vajo, C.C. Ahn, Saturation of hydrogen sorption in zn benzenedicarboxylate and Zn naphthalenedicarboxylate, J. Phys. Chem. B. 110 (3) (2006) 1099–1101.

[46] Y.K. Hwang, J. Chang, S. Park, D.S. Kim, Y. Kwon, S.H. Jhung, et al., Microwave fabrication of MFI zeolite crystals with a fibrous morphology and their applications, Angew. Chem. – Int. Ed. 44 (4) (2005) 556–560.

[47] A. Loupy (Ed.), Microwaves in Organic Synthesis, First Edition, Wiley-VCH, 2002, 499 p.

[48] P. Potiyaraj, P. Kumlangdudsana, S.T. Dubas, Synthesis of silver chloride nanocrystal on silk fibers, Mater. Lett. 61 (11–12) (2007) 2464–2466.

[49] S. Hermes, F. Schröder, S. Amirjalayer, R. Schmid, R.A. Fischer, Loading of porous metal-organic open frameworks with organometallic CVD precursors: inclusion compounds of the type [LnM]a@MOF-5, J. Mater. Chem. 16 (25) (2006) 2464–2472 (cited 31 May 2010).

[50] L. Huang, H. Wang, J. Chen, Z. Wang, J. Sun, D. Zhao, et al., Synthesis, morphology control, and properties of porous metal-organic coordination polymers, Micropor. Mesopor. Mater. 58 (2) (2003) 105–114.

[51] D. Saha, Z. Wei, S. Deng, Hydrogen adsorption equilibrium and kinetics in metal-organic framework (MOF-5) synthesized with DEF approach, Sep. Purif. Technol. 64 (3) (2009) 280–287.